

An Early Warning System for Asteroid Impact

John L. Tonry⁽¹⁾

ABSTRACT

Earth is bombarded by meteors, occasionally by one large enough to cause a significant explosion and possible loss of life. It is not possible to detect all hazardous asteroids, and the efforts to detect them years before they strike are only advancing slowly. Similarly, ideas for mitigation of the danger from an impact by moving the asteroid are in their infancy. Although the odds of a deadly asteroid strike in the next century are low, the most likely impact is by a relatively small asteroid, and we suggest that the best mitigation strategy in the near term is simply to move people out of the way. With enough warning, a small asteroid impact should not cause loss of life, and even portable property might be preserved.

We describe an “early warning” system that could provide a week’s notice of most sizeable asteroids or comets on track to hit the Earth. This may be all the mitigation needed or desired for small asteroids, and it can be implemented immediately for relatively low cost.

This system, dubbed “Asteroid Terrestrial-impact Last Alert System” (ATLAS), comprises two observatories separated by about 100 km that simultaneously scan the visible sky twice a night. Software automatically registers a comparison with the unchanging sky and identifies everything which has moved or changed. Communications between the observatories lock down the orbits of anything approaching the Earth, within one night if its arrival is less than a week. The sensitivity of the system permits detection of 140 m asteroids (100 Mton impact energy) three weeks before impact, and 50 m asteroids a week before arrival. An ATLAS alarm, augmented by other observations, should result in a determination of impact location and time that is accurate to a few kilometers and a few seconds.

In addition to detecting and warning of approaching asteroids, ATLAS will continuously monitor the changing universe around us: most of the variable stars in our galaxy, many microlensing events from stellar alignments, luminous stars and novae in nearby galaxies, thousands of supernovae, nearly a million quasars

¹Institute for Astronomy, University of Hawaii

and active galactic nuclei, tens of millions of galaxies, and a billion stars. With two views per day ATLAS will make the variable universe as familiar to us as the sunrise and sunset.

Subject headings: asteroid, asteroid impact, sky survey

1. Introduction

In recognition of the hazard posed to the Earth by asteroid impact, Congress has mandated that NASA undertake a Near Earth Object (NEO) survey program to detect, catalog, and track NEOs of 140 m diameter and larger. The recent passage of a 7 m diameter asteroid 2009 VA in Nov 2009 within only one Earth diameter emphasizes that this is a real threat, and the fact that only a small fraction of such close passages are detected reminds us that we are in fact in a continuous storm of small asteroids passing close by. In the previous year, the Earth was struck by 2008 TC3 on 7 Oct 2008 in the Sudan. (A description and references can be found at the JPL NEO website, neo.jpl.nasa.gov/news/2008tc3.html.) Perhaps more disturbing, on October 8, 2009 a ~ 50 kton atmospheric explosion occurred over Indonesia that is thought to have been caused by a ~ 10 m asteroid impacting the atmosphere. (The JPL description is at neo.jpl.nasa.gov/news/news165.html.)

The article by Asphaug (2009) reviews what is known about asteroid populations and characteristics. (We use the term “asteroid” to mean any small solar system body, asteroid, comet, meteor, etc.) The population of asteroids is quite well known as a function of brightness, usually characterized by the H magnitude (V band magnitude the asteroid would have at 1 AU distance from both the Sun and observer, viewed at opposition). The number of main belt asteroids goes approximately as the -2.5 power of size, but the number of small (< 200 m) NEOs reported by Brown et al. (2002) goes more like the -4 power of size. Since the arrival impact energy goes as the cube of the asteroid size the net arrival energy is more or less uniform per logarithmic size interval.

Conversion from observed population to surface destruction involves an estimate of albedo to derive size (usually taken as a weighted average of ~ 0.14 combining ~ 0.20 for the S-type asteroids that predominate among NEOs and ~ 0.05 for the C-type that are the most numerous in the Solar System), an estimate of density to derive mass (usually taken as $\sim 2-3$ g cm $^{-3}$ for S-type, although ice-dominated comets have a density less than water, C-type are ~ 1.5 g cm $^{-3}$, and M-type may have a density in excess of 6 g cm $^{-3}$), an estimate of arrival velocity (typically ~ 15 km s $^{-1}$, but there is a broad distribution), and an estimate of the fraction of energy that couples through the atmosphere to ground destruction. An

asteroid of H magnitude of 22 is therefore taken to have a diameter of 140 m and to carry about 100 Mton of kinetic energy. Morbidelli et al. (2002) perform this calculation in much more detail and fidelity.

The atmosphere has a surface density equivalent to about 10 m of water so we can expect that an impactor must be *considerably* larger than ~ 10 m before a substantial fraction of its kinetic energy reaches the ground instead of being dissipated in the atmosphere. For example, Melosh and Collins (2005) calculate that the ~ 30 m iron impactor that created the 1.2 km Meteor Crater in Arizona delivered only ~ 2.5 Mton to the ground of ~ 9 Mton of arrival kinetic energy.

Boslough and Crawford (2008) performed a detailed hydrocode calculation of low-altitude airbursts from asteroid impact, using the Tunguska explosion that flattened trees over an area of ~ 1000 km² in 1908 as a calibrator, and found that it is not a good assumption to compare an asteroid impact to a stationary point explosion (e.g. nuclear bomb test) at the altitude where the asteroid explodes. One difference is that the wake from the incoming object creates a channel by which the explosion is directed upward, and even a few Mton explosion will rise hundreds of kilometers into space. Another difference is that the incoming momentum carries the fireball and shock wave much lower than an equivalent point explosion, causing commensurately more damage on the ground. They also performed a calculation of the effects of a 100 Mton stony impactor and found that although the asteroid explodes before it hits the ground, the fireball touches down over a diameter of 10 km with temperatures in excess of 5000 K for 10 seconds.

The 2007 impact in Carancas, Peru of a relatively small (~ 3 m, 1 ton kinetic energy) chondrite left a 13 m crater. This seems to indicate that there are mechanisms by which a small impactor can couple significant energy to the ground, although most, like 2008 TC3 or the explosion over Indonesia in 2009, will explode harmlessly, high in the atmosphere.

We are therefore left with some uncertainty about the frequency of damage from asteroid impact. The calibration by Brown et al. (2002) of small NEOs is based on the rate of large fireballs from atmospheric impacts and a conversion from optical to explosion energy, and this is joined onto estimates from counts of asteroids as a function of H magnitude. The rate of impacts by large asteroids (140 m and larger) is estimated to only one per 20,000 years or more, the rate of impacts by 50 m, Tunguska-sized objects (5 Mton arrival kinetic energy) is about one per 1,000 years, and the rate of 10 m (40 kton arrival kinetic energy) impacts is about one per decade (NRC report, 2010). These rates are probably uncertain to a factor of at least two, and the work of Boslough and Crawford illustrates the difficulty in predicting surface damage from the incident kinetic energy.

The NASA NEO Report (2007) found that a combination of planned surveys by Pan-STARRS-4 and LSST could reach 83% completeness for 140 m diameter NEOs by 2026. The total architecture cost was estimated at about \$500M in FY06 dollars. In order to speed up and improve the detection probability, NASA found that an additional \$800M to \$1B for either an additional LSST system dedicated to potentially hazardous object (PHO) detection or a dedicated space imager could bring the completion limit to better than 90% by 2020.

This conclusion was affirmed in the recent report by the NRC report “Defending Planet Earth: Near-Earth Object Surveys and Hazard Mitigation” (2010) on survey and mitigation strategies that NASA might pursue to reduce the risk from hazardous objects, but they stressed the severe tension between cost and survey completion deadline, and suggested that 2030 may be a more attainable goal, although still at high cost. The NRC report also recognized that the damage from relatively small asteroids in the 30–50 m range may be greater than heretofore appreciated, and recommended that “surveys should attempt to detect as many 30–50-meter objects as possible”.

We believe that, while the final solution of finding, cataloging, and tracking 90% of asteroids of 140 m is very hard, the technology to find most asteroids of 50 m or larger on their final approach is now in hand. Although this may not give us enough warning to mount a mission to deflect the asteroid, it should give us enough warning to know exactly where and when the impact will occur. Lives can be saved by moving out of the impact area or away from the tsunami run-up, even though loss of property is unavoidable.

We describe how the construction and operation of a new sky survey could continually scan the visible sky. This facility, entitled “Asteroid Terrestrial-impact Last Alert System” (ATLAS) would use an array of eight wide-field, fast telescopes equipped with large detector arrays to scan the visible sky ($\sim 20,000$ sq deg) twice per night. Its sky completeness gives us a better than 50% chance of detecting any 50 m asteroid approaching from a random direction, and its sensitivity provides three week’s warning of 140 m objects and one week for 50 m asteroids.

The second section discusses the meaning of “etendue” generally, and presents equations for “survey capability” and signal to noise (SNR) achievable from a survey instrument, even in the regime of undersampled pixels. This lays the foundation for evaluation of how scientific goals can be met by a given survey implementation. The third section presents details of the ATLAS concept and describes how it compares with other surveys, present and planned. The fourth section describes how ATLAS performs in its role of detecting hazardous asteroids as well as other science topics. We find that ATLAS has some very interesting capabilities beyond early warning and is quite complementary to other existing or planned surveys. We

conclude with thoughts on how ATLAS could provide the seed for a “World-Wide Internet Survey Telescope” that could improve the probability of detection and the warning time of approaching impactors.

2. Etendue and Survey Design

2.1. Etendue and information

The technical term “etendue” means the product in an optical system of the solid angle and cross-sectional area occupied by the bundle of light rays. Liouville’s theorem guarantees that this product is conserved throughout the optical system, provided there is no absorption. In particular, at the entrance aperture, the product of solid angle seen on the sky times the collection area is a measure of how large the “grasp” of an optical system is. This “etendue” product is therefore often adopted as a measure of the merit of proposed survey systems, with some understanding that it has something to do with the rate at which scientific value can be accrued.

The information content in N independent measurements at signal to noise ratio (SNR) S is expressible in $N \log_2(S)$ bits. If our science goal is to generate a catalog of independent quantities, this might be an appropriate metric for the trade-off between quantity N against quality S to maximize information. However, an important and common science goal is accumulation of SNR for a measurement to which many correlated observations contribute. In this case the science value lies in the SNR of the sum or other combination of measurements that are presumed to be highly correlated, and the information content goes as $\log_2(N^{1/2}S)$, or $\sum \frac{1}{2} \log_2(n_i S_i^2)$ if we do this for a number of classes of inquiry, collecting n_i objects in each class with SNR S_i . Colloquially, the net SNR from averaging N measurements improves as $N^{1/2}$.

This sum, $\log(n_i S_i^2)$, is in fact the standard metric that is used to evaluate the capability of a survey system. It is not unique, nor is it appropriate for all scientific goals (for example it does not optimize detection rate of stellar occultations by hot Jupiters, where the dependency of capability on S_i is essentially a step function at $S_i \sim 200$), but it does describe the main scientific purposes to which survey data are usually applied. We will use the term “capability” henceforth to mean “accumulation of $\log(n_i S_i^2)$ per unit time” in order that “etendue” can be reserved for its technical use.

In the Poisson limited case, where the variance is proportional to the number of photons collected and n_i is proportional to the solid angle surveyed, $(n_i S_i^2)$ does not depend on how survey time is apportioned between area coverage and depth – capability is basically the

number of photons collected from objects of class i regardless of which objects the photons come from. There are two curbs on this covariance, apart from the details of luminosity function or spatial distribution. The first arises when systematic error at extremely low or high S_i (e.g. “read noise” or “flatfielding error”) slows the growth of information from $n_i^{1/2}$ – it is often not practical to increase n_i without bound by permitting S_i to become arbitrarily small, nor do we necessarily gain by arbitrarily increasing S_i on a single object. The second limit arises when n_i becomes so large within a solid angle that objects blur together – their perceived fluxes are no longer independent, which again limits the growth of information. If we assign a footprint solid angle ω to an object blurred by the point spread function (PSF) and consider an object to have value only if no other object’s footprint overlaps its center, the maximum density of isolated objects is achieved when the overall number density is ω^{-1} , at which point the density of non-overlapped objects is lower by the natural logarithm base, $(e\omega)^{-1}$.

Apart from these considerations, and for known objects with sufficient density on the sky or randomly positioned objects, maximizing n_i is tantamount to maximizing the solid angle that can be observed per unit time. Therefore we can consider the survey metric to be ΩS_i^2 , where Ω is the survey solid angle, but remembering that this is not valid when S_i is low enough to be affected by systematics or when the PSF and object footprint is large enough that objects start to overlap. The survey capability is the rate at which ΩS_i^2 is accumulated.

2.2. SNR and PSFs

Recovery of an unresolved object’s flux in the face of blurring and noise is a finely honed art. For uniform, independent Gaussian noise the optimum SNR occurs by cross-correlating (often mis-named convolving) the image with the PSF. More generally, the optimum cross-correlation kernel is just the Wiener filter, whose Fourier transform (FT) depends on those of the PSF, $P(k)$, and the noise, $N(k)$: $|P|^2/(|P|^2 + |N|^2)$. In the limit that an object is faint compared to the noise the optimum kernel then devolves to the PSF itself, but if the object’s noise variance is significant or if the background noise is correlated (e.g. by rebinning) the optimal kernel becomes narrower in image space.

Note that this is true for undersampled images as well, where it is understood that the kernel is the convolution of a “physical PSF” (meaning distribution of delivered flux prior to integration within a pixel) with a detector pixel *with phase shift*, i.e. the optimal kernel depends on the exact sub-pixel position where the object lies.

The net SNR from a faint point source of total flux f spread over a unity integral PSF

P , in the face of independent, Gaussian noise variance per unit area (square arcsec, for example) σ^2 , derived from integration against a unity integral kernel K is just

$$\text{SNR} = \frac{f}{\sigma} \frac{\int KP}{[\int K^2]^{1/2}} = \frac{f}{\sigma} [\int P^2]^{1/2}, \quad (1)$$

where the right side expresses the SNR when the PSF is used as an optimal kernel.

We integrated equation 1 for a variety of popular PSF models, with results from the well-sampled regime given in Table 1. Since $[\int P^2]^{1/2}$ for a given PSF must be inversely proportional to the spatial scale in order to maintain unity integral, the SNR will be proportional to $f/\sigma d$, where we use the full width half maximum (FWHM) d as a convenient measure of the PSF extent. We see that aperture photometry delivers an SNR that is about 12% worse than PSF integration.

Table 1: SNR for different PSFs

PSF	α_{PSF}	α_{circ}	r_{circ}	Atm?
Gaussian	0.66	0.60	0.70	N
Kolmogorov	0.57	0.51	0.71	Y
Moffat	0.58	0.51	0.73	Y
Waussian	0.52	0.45	0.76	Y
Cubic Lorentzian	0.40	0.28	0.84	N

Notes: The profiles are Gaussian, a Kolmogorov $\exp(-k^{5/3})$ profile, a Moffat (power of a Lorentzian) profile $(1 + r^2)^{-\beta}$ with $\beta = -4.765$ recommended by Trujillo et al. (2001), a ‘‘Waussian’’ (wingy Gaussian) $(1 + r^2 + r^4/2 + r^6/12)^{-1}$ introduced by Schechter et al. (1993) for DoPhot, and a cubic Lorentzian (i.e. Moffat function with $\beta = 3/2$). The second column is the proportionality factor (SNR $\sigma d/f$) for a PSF kernel, the third column the factor for an optimal circular, top-hat kernel, the fourth column the optimal top-hat radius in units of d , and the fifth column indicates which PSF profiles are realistic approximations to atmospheric PSFs.

We also performed these integrations into the extremely undersampled regime, averaging SNR^2 over PSF position within a square pixel, and found that a reasonable fit to the results for the middle three (atmospheric) PSFs from Table 1 is

$$\text{SNR} = \frac{f}{\sigma} (3.5d^2 + 0.4dp + p^2)^{-1/2} \quad (2)$$

where d is the *physical* FWHM, p is the pixel size, σ^2 is the background noise variance per unit area, and f is the total flux in the faint point source. Equation 2 is therefore a good approximation for atmospheric PSFs, regardless of undersampling.

An application of equation 2 is selection of pixel size for optimal SNR, trading off read noise against background noise variance. (For zero read noise the optimum is an infinitely small pixel.) If we add σ_R^2/p^2 to σ^2 , where σ_R is the read noise per pixel, we can solve for the pixel size that maximizes the SNR. An approximate solution to the quartic equation is given by

$$p_{opt}^2 = 2d \sigma_R / \sigma. \quad (3)$$

Since σ_R/σ is the pixel size at which the read noise equals the sky noise, the pixel that optimizes photometry SNR is $\sqrt{2}$ times the geometric mean of the physical FWHM and the size that balances read noise against sky noise (which depends on bandpass and sky brightness).

2.3. Survey design and performance

A survey system’s ability to capture photons from a source depends on its aperture and obstruction, vignetting, filter bandwidth and throughput, atmospheric throughput, detector quantum efficiency and fill factor which we bundle into a single throughput number ϵ . Operationally, we use the zeropoint of the AB magnitude system, 5.48×10^6 photons $\text{cm}^{-2} \text{sec}^{-1} \ln(\nu_2/\nu_1)^{-1}$, to find that an AB magnitude of $m_0 = 25.10$ provides one photon per m^2 per sec per bandpass of 0.2 in natural log of wavelength (a typical width for astronomical filters). We define ϵ as the factor by which an actual system falls short of this ideal (or conceivably exceeds it by using a broader bandpass), i.e. the signal from a source of magnitude m captured by an aperture of area A is

$$f = A \epsilon t_{exp} 10^{-0.4(m-m_0)}. \quad (4)$$

We define the net fraction of shutter open time, including losses for weather, daytime, instrumental failures, etc. as “duty cycle”, δ . A survey system’s temporal efficiency depends on the net exposure time devoted to a given field, t_{exp} , adding together however many successive dithers are deemed necessary, and the matching overhead time t_{OH} that adds all proportionate times such as read out, slew, focus, etc. We term the ratio $t_{exp}/(t_{exp} + t_{OH})$ the “temporal duty cycle” δ_t . δ can have an interesting relation to δ_t , especially when one considers sites in Antarctica ($\delta = \delta_t$ in the winter), in orbit, or an “observatory” that consists of many units at a diversity of geographical location, but generally speaking we have control over δ when designing a survey but control over only δ_t when operating a survey (by changing t_{exp}).

Let us define the “PSF footprint” ω as the solid angle that carries background noise equal to f/SNR for a faint point source of flux f and SNR defined by the flux measurement

algorithm in use (e.g. those in Table 1), so that we can calculate SNR for a given object by comparing its total flux to the noise found in this “PSF footprint”. Equation 2 gives this solid angle as $\omega = (3.5d^2 + 0.4dp + p^2)$ for the case of PSF-matched photometry with a atmospheric seeing profile, independent noise, but not necessarily well sampled.

If μ is the sky brightness per square arcsecond, the noise variance that the signal contends with is

$$\sigma^2 = A \epsilon t_{exp} (\omega 10^{-0.4(\mu-m_0)} + 10^{-0.4(m-m_0)}) + f_R^2, \quad (5)$$

where f_R^2 is the readout variance over ω ’s worth of pixels: $f_R^2 = \sigma_R^2 p^{-2} \omega$ for a read noise of σ_R e⁻ and pixel size p arcsec.¹

Equations 4 and 5 provide the square of the signal to noise ratio, S_1^2 for at this particular magnitude:

$$S_1^2 = A \epsilon t_{exp} \omega^{-1} 10^{+0.4(\mu-m_0)} 10^{-0.8(m-m_0)} [1 + 10^{-0.4(m-m_{sky})} + f_R^2 f_{sky}^{-1}]^{-1}, \quad (6)$$

where m_{sky} is sky magnitude within ω , $m_{sky} = \mu - 2.5 \log \omega$, and f_{sky} is equivalent flux in e⁻, $f_{sky} = A \epsilon t_{exp} 10^{-0.4(m_{sky}-m_0)}$. In this equation and below, the term in square brackets is approximately unity when the sky noise dominates the object’s photon statistics and the read noise; we include it here for completeness, but drop it henceforth for clarity. It can be reintroduced if the read noise or object photon noise is significant with respect to the background noise, and it causes the turn-down in the curves of Figure 2

The capability metric defined above includes a factor for the surveyed solid angle. The cadence time t_{cad} to carry out t_{exp} worth of integration over a survey solid angle Ω is related to the field of view solid angle Ω_0 and duty cycle by

$$\Omega t_{cad}^{-1} = \Omega_0 t_{exp}^{-1} \delta. \quad (7)$$

Therefore the capability function at magnitude m is

$$\frac{S_1^2 \Omega}{t_{cad}} = \frac{A \Omega_0 \epsilon \delta}{\omega} 10^{+0.4(\mu-m_0)} 10^{-0.8(m-m_0)}, \quad (8)$$

This includes the $A\Omega_0$ term commonly called “etendue”, but also the dependence on ω , ϵ , δ , and μ that are crucial to the real SNR gathering capability of a system. Rewriting the system-fixed parameters as an overall system capability M , equation 9 reveals how the

¹Note that the term involving the object’s magnitude m itself is somewhat notional – not only does the weighting involve $\int P^3$ for the case of a PSF kernel, but the optimal kernel would change for objects that are brighter than noise. Its presence serves to remind us that SNR depends on the Poisson statistics of the flux from the object itself.

survey choices of cadence, SNR, survey area, and magnitude can be traded off against one another.

$$M = \frac{A \Omega_0 \epsilon \delta}{\omega} 10^{+0.4(\mu+m_0)} = \frac{S_1^2 \Omega}{t_{cad}} 10^{+0.8m}. \quad (9)$$

Taking a logarithm, survey-variable parameters on the right add to the (nearly) constant left hand side:

$$\log M = 0.8m - \log t_{cad} + \log \Omega + 2 \log S_1. \quad (10)$$

This relation forms a surface in the observability space of magnitude m , SNR, solid angle, and cadence interval that is accessible for a particular survey capability. The left hand side is not strictly fixed; changing t_{exp} affects δ_t and δ as well as the (dropped) term in square brackets if the read noise is not negligible, and the term in square brackets also contributes if the object is brighter than the background. A sketch of how the left hand side is affected is illustrated in Figure 1. Apart from this, the “observability surface” is a plane in log space.

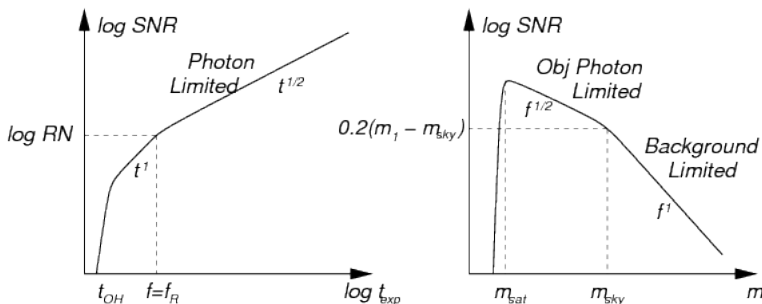


Fig. 1.— SNR, illustrated by cuts at constant magnitude and t_{exp} , falls precipitously when t_{exp} approaches the overhead time t_{OH} ($\delta_t \ll 1$) or the magnitude approaches the saturation limit m_{sat} (which depends on t_{exp} of course), falls quickly with exposure time when the flux is less than the read noise f_R , and transitions between photon and background limited when the magnitude becomes fainter than the background magnitude m_{sky} within a PSF.

As argued in the section above, most science value is not changed by tradeoffs that keep the product ΩS_1^2 constant. In practice scientists tend to set S_1 at a fixed, minimum value for which systematics are not compromising the SNR and then maximize survey solid angle Ω . For moving object detection S_1 might be 5; for Type Ia supernova light curves S_1 might be 30 at peak; for planetary occultations S_1 might be 200. This “science value level set” or SNR operating point provides second constraint in observability space for a survey. Therefore there are really only two independent parameters for setting a given survey’s operation for a given capability: for a given magnitude the cadence time dictates the solid angle.

The density of various types of objects and application of science values can now optimize the overall survey capability. For example if value lies in detection of orphan afterglows of gamma ray bursts (GRB) we may choose to spend our M capability in short t_{cad} and large Ω at the expense of m . If value lies in detection of planetary occultations of stars we cannot give up S_1 or t_{cad} and therefore may make compromises in m or Ω . Searching for solar system objects would emphasize m and Ω at the cost of minimal S_1 and allowing t_{cad} to grow to the linking confusion limit. General purpose surveys such as PTF, Pan-STARRS, and SkyMapper strive to maximize capability M generally, but then dedicate portions of time (subdivide δ) to different locations in the observability surface according to different science goals. LSST has claimed to be able to maximize science value at a fixed location on the observability surface, but of course it is straightforward to move on the surface or split time into different surveys should that prove desirable.

3. ATLAS

Spaceguard has discovered most NEOs larger than 1 km, and has determined that none will strike the Earth in the foreseeable future. The NRC report (2010) estimates that the remaining fatality rate is bimodal as a function of impactor size, with a 10^{-6} yr $^{-1}$ probability of impact by a 1–2 km object that would cause 50 million deaths (averaging over possible impact locations), and a 10^{-3} yr $^{-1}$ probability of impact by a ~ 50 m object that would cause an average of 30,000 deaths. The H magnitude of a 50 m asteroid is 24 or fainter, and for a typical phase function the actual magnitude at 1 AU distance will be >25 – 26 . This suggested to us that surveying at a much smaller distance than 1 AU would make sense, and by definition any Earth-impacting asteroid will be present shortly before impact at a small distance. Choosing one week as a minimum warning interval for civil defense against a limited explosion and three weeks warning as necessary for a city-devastating explosion, we were surprised to discover that this places rather modest requirements on limiting magnitude, although it does require isotropic vigilance.

It is possible to achieve the requisite sensitivity over half the sky with survey hardware that is more or less off-the-shelf and of modest cost. We have proposed ATLAS to NASA for construction and two years of operation; fundamentally the system is equivalent to a telescope of 0.5 m aperture with a 40 sq deg field of view, subjected to an effective PSF of $3.8''$, with bandpasses twice as wide as an SDSS filter. By comparison, the Palomar Transient Factory uses a 1.2 m aperture, an 8 sq deg field of view, SDSS filters, and enjoys $\sim 2.2''$ seeing for a very comparable capability.

The NASA proposal implements ATLAS using eight Takahashi astrographs of 0.25 m

aperture and 0.7 m focal length that each provide a 20 sq deg field of view. These telescopes are small enough that there are a number of equatorial mounts available commercially that can carry more than one telescope. We believe that a fully equipped telescope with focuser, filters, shutter, camera adapter and mount should cost about \$50k.

The cameras for ATLAS each have a 4×4 k pixel focal plane, taking advantage of an existing inventory of 2×4 k CCDs with 15 μm pixels. Although the pixel size is not optimal in the sense above (a 10 μm pixel provides about 0.1 mag more sensitivity in moderate seeing), a pair of those CCDs could be mounted in a cryostat and equipped with a controller for a unit cost that we again believe will be about \$50k (since there is no detector cost).

ATLAS consists of a set of eight of these telescope and camera units, and reaches an interesting survey capability level, while remaining cost effective. While subject to further optimization, the design reference calls for

- Exposures of $t_{exp} = 30$ sec with $t_{OH} = 5$ sec and $10 e^-$ read noise, using broad filters that are approximately $g+r$ and $r+i$. (The science program of finding asteroids calls for the broadest possible filters; the other science programs benefit from color information.)
- Four unit telescopes are clustered on a common mount within an observatory, and the other four in an identical observatory separated by ~ 100 km in order to obtain good parallaxes to 0.1 AU, enabling instantaneous alerts for approaching objects as well as providing the crucial function of weeding out false alerts from space junk. The “blue” observatory uses the $g+r$ filter set; the “red” observatory the $r+i$ filters. At each observatory telescopes are used as two co-aligned pairs, thereby providing 40 sq deg of instantaneous field of view at twice the aperture of a single telescope and twice the throughput of a single SDSS filter. The two observatories synchronize their pointing and observations exactly.
- Both observatories cover the entire, visible sky (20,000 sq deg) twice per night, visiting each point with a time separation of about 1 hour (RA permitting) in order to obtain unambiguous tracklets of moving objects.

Although the 15 μm pixels subtend $4.4''$ and are therefore considerably undersampling the PSF, a detailed calculation of the expected sensitivity is promising. A single, moonless exposure in either bandpass by each of the telescopes reaches SNR 5 at $V = 19.1$ for a solar spectrum. The seeing assumed for this was $1.5''$, but the SNR is relatively insensitive because of the undersampling and the contribution from optics blur. The sum of the images from a co-aligned pair of units therefore yields SNR 5 at $V = 19.5$. The combination of the observations from the two co-aligned pairs at the two observatories provides SNR 5 at $V = 19.9$. (The two filters are chosen to provide the same SNR for a solar spectrum.)

ATLAS’s performance on objects fainter than this depends on the details of the object and how the observatories can communicate. Our design calls for each observatory to have

a cluster of computers that can align and co-add images, and can reliably detect objects at SNR 3.7 (with false alarms). We demand that the observatories have at least enough bandwidth that they can share detections, so as to confirm SNR 3.7 detections and reach SNR 5 at $V = 19.9$.

We cannot expect to detect moving objects (or objects closer than 0.05 AU with a significant parallax) much fainter than $V \sim 20$ since they will not align on successive images. However, stationary objects that are observed twice per night will be detected at SNR 5 at $V \sim 20$ in both the red and blue bandpasses, or SNR 5 at $m = 20.35$ in a combination of red and blue images. Obviously detections of stationary objects can continue to fainter magnitudes by stacking many night’s observations until systematics dominate.

With no defocus, the cameras will saturate at $V \sim 12.5$ (blue) and $V \sim 13$ (red). We intend to equip each observatory with a pair of high-end digital SLR cameras to provide 5 color photometry to a limiting magnitude of $V \sim 6$, so as to be able to monitor brighter stars and extend the dynamic range for very bright transients.

4. Ongoing and Planned Surveys

There are many past, ongoing, and future sky surveys for a variety of purposes. Table 2 shows the basic design choices made by a set of successful efforts and some proposed ones.

The most productive asteroid and near Earth object (NEO) search programs are currently the Catalina Sky Survey (Larson et al., 2003; www.lpl.arizona.edu/css), LINEAR (Stokes et al., 2000; www.ll.mit.edu/LINEAR), and Spacewatch (McMillan et al., 2006, Larson et al., 2007; spacewatch.lpl.arizona.edu). The JPL website (neo.jpl.nasa.gov) attributes 73% of asteroid discoveries in 2009 to Catalina (60% of NEOs), 14% to LINEAR (28% of NEOs), and 8% to Spacewatch (4% of NEOs). (Spacewatch is now spending a greater fraction of time on follow-up rather than discovery.)

“Pi of the Sky” (Malek et al, 2009; grb.fuw.edu.pl) is a representative GRB search program. RAPTOR (Vestrand et al., 2003; www.raptor.lanl.gov) is another interesting example of GRB and other transient search, but is not listed in Table 2. These projects put a high premium on rapid cadence and rapid follow up capability, at the cost of limiting magnitude.

“SuperWasp” (Pollacco et al. 2006; <http://www.superwasp.org>) and “HAT-South” (Bakos et al. 2009; www.cfa.harvard.edu/~gbakos/HS) are examples of surveys searching for planetary occultations. Such surveys must work at very high SNR at fast cadence, again

at the expense of limiting magnitude, but their science does not lack for stars of suitable brightness. HAT-South is particularly interesting for comparison with ATLAS because there are marked similarities in the equipment, but the science for HAT-South and ATLAS lives in different locations in observability surface.

The Palomar Transient Factory (PTF) (Law et al., 2009; www.astro.caltech.edu/ptf) has dedicated time to different search strategies for optical transients such as supernovae. We list the properties of the “5 day” portion of their survey.

Pan-STARRS1 (Burgett & Kaiser, 2009; pan-starrs.ifa.hawaii.edu) and SkyMapper (Keller et al., 2007; rsaa.anu.edu.au/skymapper) seek to perform surveys of the entire northern and southern skies to unprecedented depths. Both surveys are optimized to find transients and moving objects. A portion of Pan-STARRS1 is dedicated to a “3pi” survey of 3/4 of the sky, revisiting once every 3 months; another portion to a “Medium Deep” (MD) survey of about 40 sq deg revisited each day to a substantial depth. We list both Pan-STARRS surveys in order to illustrate how more or less equal resources (capability) can be placed at rather different places on the observability surface. Pan-STARRS is intended to be a replicable system, with a goal of four units (PS4) sited on Mauna Kea.

The Large Synoptic Survey Telescope (LSST) (Ivezic et al., 2008; lsst.org) is proposed to survey the visible sky on a few day cadence with an 8 m telescope, projected to reach at least a magnitude fainter than Pan-STARRS1 at a much faster cadence.

Table 2 also shows how well these surveys perform and their log capability, generated from equation 9. Actual performance only correlates loosely with $A\Omega_0$: background, efficiency, and duty cycle are very serious factors. Therefore the capability is best calculated from the *right* hand side since limiting magnitude at some estimate of SNR and the overall cadence of covering a planned solid angle is generally well reported. For systems which are not yet operational we take their estimated SNR and magnitude at face value, but delivered ϵ , δ , and especially ω may fall short of pre-operational claims.

Different survey choices can trade off m , S_1 , t_{cad} , and Ω against one another on the observability surface; Figure 2 shows a cut at constant $S_1 = 5$ in the $m - t_{cad}$ plane, with point area proportional to Ω , and another cut at $S_1 = 5$ and $\Omega = 1000$ sq deg. The cadence time is defined as the mean time required to survey Ω , but the survey may include a great deal of valuable temporal sampling when the survey includes multiple exposures. For example, the PS1-3pi survey is specifically designed to detect moving objects with pairs of exposures on a ~ 15 min interval. It is therefore not safe to conclude that t_{cad} listed in Table 2 is the shortest time interval for detection of motion or variability.

Table 2: Sky Survey Design and Performance

Program	A	Ω_0	ω	m_{sky}	δ_t	S_1	m	n_c	t_{cad}	Ω	$\log M$
NEO search											
Spacewatch	0.51	2.9	16	18.0	0.50	3	21.7	1	0.5	150	20.8
LINEAR	1.2	2.0	30	17.3	0.80	4	19.0	1	0.3	2400	20.4
Catalina	0.27	8.2	41	17.0	0.50	4	19.5	1	0.4	800	20.1
GRB counterparts											
PioftheSky	0.13	484	25000	10.0	0.83	5	14.5	1	0.01	6400	18.8
Planet occultations											
SuperWASP	0.15	61	11000	10.9	0.88	100	12.9	1	0.02	3900	19.7
HAT-South	0.46	16	128	15.7	0.92	100	14.0	1	0.004	128	20.5
Sky Survey and Transients											
PTF-5day	0.85	7.8	16	18.0	0.67	5	21.4	2	5	3200	21.3
SkyMapper	1.1	5.2	8	18.7	0.88	5	22.4	6	270	20000	21.2
PS1-3pi	1.8	7.5	3.7	19.6	0.75	5	23.3	5	90	20000	22.4
PS1-MD	1.8	7.5	3.7	19.6	0.98	5	24.7	5	4	45	22.2
Proposed Surveys											
ATLAS	0.29	20	46	16.9	0.86	5	19.9	2	0.7	20000	21.8
PS4-3pi	7.1	7.5	3.0	19.8	0.92	5	23.6	5	10	20000	23.6
LSST	35	9.6	2.9	19.8	0.88	5	24.5	2	3	10000	24.5

Notes: A is the net aperture in m^2 , including obscurations and the number of units; Ω_0 is the solid angle in deg^2 per exposure; ω is the noise equivalent PSF area in arcsec^2 as discussed in the text; m_{sky} is the magnitude collected within ω when the sky brightness is $\mu = 21$ per sq arcsec; δ_t is the exposure duty cycle $t_{exp}/(t_{exp} + t_{OH})$; S_1 is the SNR achieved at magnitude m which includes the coadded sensitivity from the contributions of n_c colors; the cadence times t_{cad} in days have been adjusted for 2/3 clear weather; Ω is the actual solid angle in deg^2 surveyed in the cadence time t_{cad} ; “Catalina” is only the 0.7 m Schmidt, its combination with the Siding Spring Survey and the Mt. Lemmon Survey almost double the total capability; “PS4-3pi” presumes a 100% 3π survey for PS4, but the etendue may be split as with PS1; “LSST” is based on current suggestions for a 2-color, 2π survey which is estimated to reach $m = 24.5$ in 3 days, including weather.

It is instructive to examine how the ATLAS proposal differs from HAT-South and Pan-STARRS1. ATLAS is using a very similar approach to the HAT-South project, even to the extent of both using four Takahashi telescopes on common mounts, each feeding a $4 \times 4k$ camera. ATLAS gains factors in capability from ϵ ($\times 4$), ω ($\times 3$), Ω ($\times 1.5$), but loses in A ($\times 0.7$) for a net gain of about an order of magnitude. Pan-STARRS1 and ATLAS have nearly the same product of $A\Omega_0\epsilon$ (collect photons at the same rate), but of course Pan-STARRS1 has about an order of magnitude higher capability than ATLAS because ω is so much smaller.

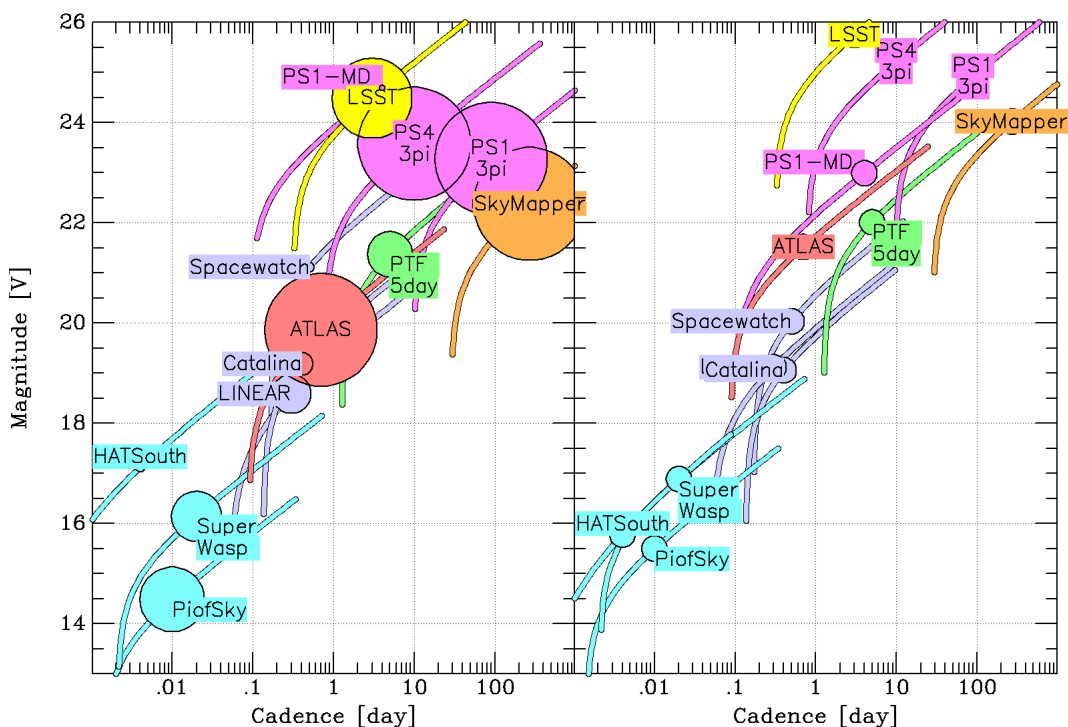


Fig. 2.— The various system’s capabilities are shown at common $\text{SNR} = 5$ in the magnitude-cadence plane on the left. The area of the symbol is proportional to the solid angle Ω surveyed in that cadence time, and the lines illustrate the observability surface in m and t_{cad} at fixed Ω and SNR . However, putting all surveys at a common $\text{SNR} = 5$ does some injustice to the science they seek to achieve. The rolloff in magnitude occurs when t_{exp} becomes comparable to t_{OH} (the square bracket term). On the right, the various systems capabilities are shown in the magnitude-cadence plane at common $\text{SNR} = 5$ and assuming they trade off sensitivity for coverage to $\Omega = 1000$ sq deg.

It is not worthwhile to try to split hairs about which survey is the “best” or most capable; many of the parameters in the table above are rough enough that it is not possible to make an accurate comparison. Even more important, the table fails to clarify all the factors which make the various surveys especially well tuned for the science they are trying to do. However, ATLAS does occupy an important portion of design space. It is an order of magnitude faster than existing NEO surveys, it reaches much fainter magnitudes than the other sub-day cadence surveys, and it is unique in surveying the entire sky several times per night. While some of the other systems could move at constant capability to cover the entire sky nightly, they would not be able to do so at nearly the sensitivity of ATLAS.

ATLAS is complementary to general surveys such as Pan-STARRS, SkyMapper, and LSST. Like these it covers most of the sky, but it offers a much faster cadence at the cost of less sensitivity, fewer colors, and less resolution. As described in the next section, there is a great deal of science to be found in this brighter, faster regime of discovery space in addition to the primary mission of finding asteroids approaching the Earth.

5. Science with ATLAS

5.1. Asteroid Impacts

ATLAS is first and foremost a system to warn of incoming objects that might hit the Earth. ATLAS is not optimized to find objects at 1 AU and $H \sim 20$, many of which are known and will never strike the Earth. Other systems, notably Pan-STARRS and eventually LSST, have the leisure to find and catalog these better.

Fortunately the interval between collisions of the Earth with an object of ~ 50 m or larger is many centuries, the impact at Tunguska in 1908 notwithstanding. However, the cumulative frequency of Earth impacts as a function of the size of impactor has been estimated by Brown et al. (2002) as

$$N(> D) = 37 \text{ yr}^{-1} \left(\frac{D}{1\text{m}} \right)^{-2.7} \quad (11)$$

so we can expect an impact of a 20–30 m asteroid once per century, a nearly Mton-class explosion. Although most of the incident energy will be dissipated high in the atmosphere, we have already discussed the evidence that it could cause significant damage on the ground as well.

We have developed a detailed ATLAS simulator that integrates the orbits of NEOs or impactors from Veres et al (2009), either 10,000 impactors chosen to strike the Earth randomly in location and time over the next 100 years, or the full population of 270,000

NEOs. It is important to note that Earth impactors have a different orbit distribution from NEOs or even potentially hazardous objects (PHO’s) — the impactor’s orbit distribution is shifted to smaller semi-major axis, eccentricity and inclination.² This is what makes ATLAS so effective at identifying *impactors* as opposed to generic NEOs. If an asteroid can hit the Earth, its orbit must intersect the Earth’s orbit and ATLAS’s small search volume and fast cadence is ideal for finding them.

The simulator uses ATLAS’s view of each night’s sky, schedules the observing time, examines each asteroid for visibility according to its apparent magnitude and the observation’s extinction, trailing losses, and weather, and decides that an asteroid has been “found” when it has been observed 8 times in 4 tracklets or else has an accurate parallax.

ATLAS can detect more than half of impactors larger than 50 m and almost two thirds

²An NEO is defined as an object with perihelion less than 1.3 AU and aphelion greater than 0.983 AU; a PHO is an object with $H < 22$ (diameter ~ 140 m) whose orbit passes within 0.05 AU of the Earth’s orbit; an “impactor” is an object that actually strikes the Earth within 100 years.

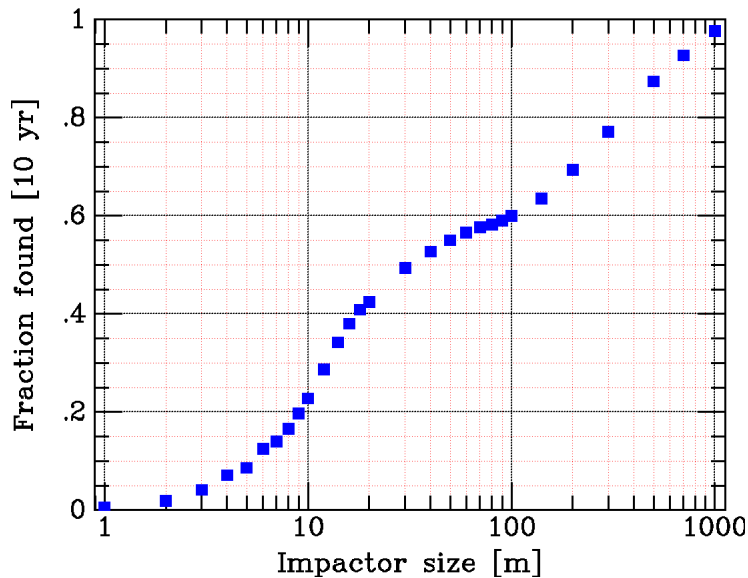


Fig. 3.— The fraction of impactors that ATLAS detects before collision is shown as a function of asteroid size for a survey of 10 years duration. The kink at ~ 20 m occurs when a significant fraction has warning time greater than one day, and the kink at ~ 140 m is caused by an increasing fraction of greater than one orbit warning times.

of 140 m impactors, as illustrated in Figure 3. The asteroids that ATLAS misses slip in from the direction of the Sun and south pole or during periods of bad weather. (An ATLAS copy in the southern hemisphere or in a different weather pattern would raise the detection fraction.) Figure 4 illustrates the distribution of warning times provided by ATLAS. Objects of 140 m diameter are typically detected 20 days before impact while 50 m diameter objects are detected with a week’s notice, when they are ~ 15 times the distance to the moon.

Simultaneous images from the two sites provide a 3σ parallax when the object is closer than 0.1 AU, about two weeks before impact. The parallax is crucial for identification of an approaching asteroid in a single night and important for vetoing confusion with space junk.

Looking at the full NEO and PHO populations, the right panel of Figure 4 shows the rate at which asteroids are found by ATLAS. ATLAS will (re)discover 50% of all 1000 m NEOs and PHOs within 1 year, 70% in 3 years, and 90% in 10 years. The net rate of detection of 140 m asteroids or larger should be more than 400 NEOs and 100 PHOs per year. ATLAS can find about 15% of all 140 m PHOs within 3 years and 30% within 10 years, slightly less than what Veres et al (2009) found for the Pan-STARRS-1 mission.

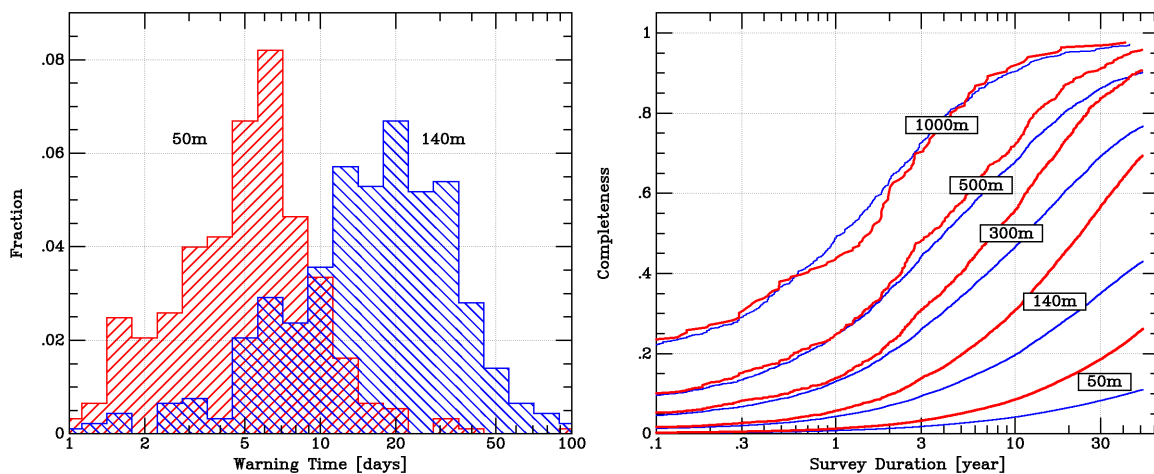


Fig. 4.— The left plot shows the distribution of warning times provided by ATLAS for impactors of 140 m and 50 m diameter that it detects. The typical 140 m impactor will be found three weeks before arrival; the typical 50 m impactor will be found one week before collision. Depending on survey duration, there is also a growing number of warning times longer than a year not illustrated here. The right plot shows ATLAS’s completeness for detection of NEOs (blue, thin lines) and PHOs (red, thick lines) of various sizes as a function of survey duration.

ATLAS is not a direct competitor for the much more capable surveys such as Pan-STARRS-4 or LSST. However, for the crucial days and weeks that an impactor is on final approach, ATLAS is far more effective than any existing NEO survey, Pan-STARRS, or LSST. The coverage and cadence that ATLAS provides gives us a high probability of seeing an incoming asteroid, and ATLAS’s sensitivity is enough to spot it while it is still reasonably distant.

When ATLAS detects a nearby object it will automatically provide the measurements to the Minor Planet Center for posting on their web-based NEO Confirmation Page. At that time, in a manner similar to the rapid followup of the first pre-impact identification of meteoroid 2008 TC₃ (Jenniskens et al. 2009), we expect other amateur and professional observers to obtain additional observations. The case of 2008 TC₃ demonstrates the amazing accuracy that can be achieved: JPL’s predictions were accurate to ~ 20 sec and ~ 100 km within hours of discovery, and the eventual prediction was accurate to ~ 1.5 sec and ~ 1 km.

5.2. Asteroid Science

ATLAS will monitor a large number of asteroids in the Main Belt as well as asteroids and comets elsewhere in the Solar System. The rapid time cadence of ATLAS is particularly well suited to providing light curves and simultaneous colors for many asteroids that can then be analyzed to infer asteroid shape and tumbling motion. ATLAS should achieve photometry in two colors with 0.01 mag accuracy at $V \sim 16$, 0.02 mag accuracy at $V \sim 17$, and 0.04 mag accuracy at $V \sim 18$. The AstDys web site (hamilton.dm.unipi.it/astdys) lists 973 numbered asteroids with $V < 16$, 3,149 with $V < 17$, and 10,078 with $V < 18$ at this moment in time (2010-10-10) in the 3/8 sky between RA 18^h and 6^h and Dec -30° to $+90^\circ$. Most are considerably off of opposition right now, so have been or will be brighter during the 4–5 months it takes to sweep by. Therefore ATLAS should provide twice-nightly two color light curves of ~ 4 month duration for at least 2,000 asteroids at an accuracy of 0.01 mag per point, 6,000 asteroids with an accuracy of 0.02 mag, and 20,000 asteroids with an accuracy of 0.04 mag.

It has been estimated by R. Jedicke (private communication) that there is a collision each day that disrupts a 10 m asteroid in the Main Belt. If the dust cloud from the collision grows to 1000 m before becoming optically thin the collision should be detectable by ATLAS. The recent asteroid collision event P/2010 A2 discovered by LINEAR achieved $m \sim 19$ and would be detectable by ATLAS.

An object in the outer solar system must have $H < 4$ to be detectable by ATLAS,

so ATLAS is unlikely to add many new discoveries to the bodies already known or that will be discovered by Pan-STARRS1. The value from ATLAS is completeness and ongoing monitoring of 3/4 of the sky. If an object has slipped between the cracks of other surveys, or happens to brighten (e.g. tumbling), or is rapidly approaching (e.g. new comets) ATLAS may be the first to discover it. The current IAU definition of a dwarf planet is a body with $H < 1$. With full illumination, at 60 AU distance (approximately the outer edge of the Kuiper belt), such a body would have a V magnitude of 18.8, and therefore be easily detectable by ATLAS. ATLAS should therefore detect virtually all dwarf planets in the solar system within one year, and be particularly useful for searching well out of the ecliptic, where such bodies might have scattered.

5.3. Supernovae

SNIa have proven utility as measures of the cosmological expansion of the universe, and it is hoped to continue with even more subtle questions such as whether the accelerated expansion is consistent with a cosmological constant. Since we do not understand very well the environment, initial conditions, trigger mechanism, and explosion process of SNIa, these extremely delicate measurements are vulnerable to systematic errors.

A Type Ia supernova at $z = 0.1$ peaks at $V = 18.9$. The ATLAS sensitivity at SNR=10 is 19.5 per day; assuming 70% clear weather, the ATLAS sensitivity for 4 nights is $V = 20.1$ for SNR=10. According to Mannucci et al. (2007) there are some 9,000 SNIa yearly closer than $z = 0.1$ (32,000 at $z < 0.15$). Since the area that ATLAS surveys each night is half of the entire sky (neglecting obscuration by the galactic plane), we can expect that ATLAS will find and follow 4,500 SNIa per year at $z < 0.1$ and SNR > 30 and 16,000 SNIa per year at $z < 0.15$ with SNR > 14 , with a 4 day sampling of the light curve. Perhaps more interesting from the standpoint of investigating systematics, ATLAS should find some 300 SNIa per year that peak at $V < 17$, and ~ 30 per year peaking at $V < 15$. This is nearly an order of magnitude greater than the discovery rate of bright SNIa over the past decade, and has the advantage of being completely unbiased. By contrast, the KAIT telescope (Li et al, 2003) finds approximately 75 supernovae per year by patrolling nearby galaxies.

The huge number of SNIa discovered by ATLAS as well as the completeness of examining the entire sky will empower us to ask questions such as characterization of explosion as a function of host galaxy properties, details of the very early phases of the explosion, and identification of outlier events that can be flagged for spectroscopy or more detailed photometry. We can also expect to see a large number of SNIa in interesting environments such as rich clusters or tidal streams of interacting galaxies.

Core collapse supernovae (CCSN) are particularly interesting when they result in a huge, collimated explosion creating a gamma ray burst. These are thought to occur in low metallicity environments from WR stars that have a high core angular momentum at time of collapse. Young et al. (2008) estimate that there are 20 CCSN per year in galaxies with $12 + \log(O/H) < 8.2$ and $z < 0.04$. ATLAS’s nightly 10σ sensitivity of $V = 19.5$ translates to $V = 18.5$ at 25σ . In 10 day’s time (7 clear nights) ATLAS achieves $V = 19.6$ at 25σ . CCSN peak at $M \sim -16.8$ (IIP), $M \sim -18.3$ (Ib/c), and $M \sim -19.6$ (IIL), and the distance modulus at $z = 0.04$ is $(m-M) = 36.2$, so ATLAS should be able to detect all of these outbursts at 25σ , extinction permitting. Since ATLAS is surveying half the sky, the expected number is 10 CCSN per year in such low metallicity galaxies.

5.4. Gravity Waves

Although LIGO has yet to detect a gravity wave (GW) event, it is virtually certain that gravity waves exist and highly likely that Advanced LIGO will detect GW events. The most common detections will be coalescing, compact objects whose changing quadrupole moment makes a vigorous, detectable “chirp” in gravity waves. Abadie et al. (2010) estimate the rates of events and sensitivities and suggest that the most likely events will be neutron star - neutron star coalescence within ~ 445 Mpc.

While in principle a coalescence of naked compact objects could give rise to minimal E&M signature, it seems quite possible that the release of more than 10^{53} ergs of energy might be accompanied by 10^{48} ergs in the optical, as argued by Stubbs (2007). Such an explosion corresponds to a luminosity with absolute magnitude of $M \sim -18$ for a duration of two days. We do not try to advocate any particular mechanism, but only make the point that if even a part in 10^{-5} of the energy release appears in the optical, it will be a substantial luminosity for a substantial duration.

Abadie et al. estimate that one NS-NS coalescence occurs every Myr in every Mpc^3 , and therefore expect to see some 40 events per year, applying a factor of 2.26 to the horizon distance of 445 Mpc to account for sky location and orientation. The distance modulus of 445 Mpc is 38.2, so an explosion of $M = -18$ would be just detectable by ATLAS, provided that it happens within the half sky visible to ATLAS and endures long enough for ATLAS to sweep across it. The nearest object that Advanced LIGO would see in one year would be a factor of $40^{1/3}$ closer, 2.7 mag brighter, and easily seen by ATLAS.

The coalescence of compact objects creates a well defined GW signal and an extremely ill-defined optical transient. On the other hand, core-collapse supernovae (CCSN) are com-

mon, and Ott (2009) has reviewed their possible GW signatures and the ability of Advanced LIGO to detect them. Advanced LIGO may be able to detect a CCSN within 1 Mpc with signal to noise of ~ 6 , but the rate of such supernovae within the Local Group is only one in ~ 20 years. There is about one CCSN each year within ~ 5 Mpc, and the rate grows rapidly at distances beyond ~ 8 Mpc that start to reach into the Virgo cluster.

CCSN closer than the Virgo cluster will be much brighter than the ATLAS magnitude limit of 20, and therefore ATLAS will detect the half of them that are in the visible sky at time of explosion. We have a decent chance over a year or two of matching an Advanced LIGO event at 3σ with a CCSN seen by ATLAS, but there is no question that ATLAS will provide times and locations for many events for which Advanced LIGO may have a $\sim 1\sigma$ detection. The time between collapse and emergence of the light flash is short enough that it should be possible to correlate CCSN events with low SNR GW events and thereby learn about the mechanism by which CCSN events create gravity waves.

5.5. Novae, Outbursts, and Variable Stars

Novae range in absolute magnitude from $M_V = -9$ to $M_V = -7$, declining by 3 mag in a week to several months, and the number per galaxy is estimated to be some 40 per year. ATLAS’s 4 day 10σ sensitivity of $V = 20.3$ gives us the ability to see novae to distance moduli of $(m-M) \sim 28$, i.e. we will certainly see all the novae in the Milky Way and M31 within ATLAS’s half sky, and most of the novae in nearby galaxies such as M81 and M101, but we will not see novae in the galaxies in the Virgo cluster.

Luminous blue variable stars flare at $M_V \sim -9$ to $M_V \sim -13$, so again, ATLAS can find and monitor many of them on a daily basis to distances as great as the Virgo cluster.

Mira variables peak at $M_V \sim -1.5$ with periods of order a hundred days, and FU Orionis outbursts peak in the range of $M_V \sim -1$, rising over a year and then declining over decades. ATLAS can monitor these all throughout the Galaxy, although M31 is too distant. A southern ATLAS would encompass the Magellanic Clouds, at distance modulus 18, so is sensitive at 10σ to $M_V = +2$ and brighter.

There are some 2000 cataclysmic variables known in the neighborhood of the Sun. ATLAS is unique in being able to keep an eye on all of them with two samples each day spread by an hour or two. This will provide excellent sampling of their periods (typically about an hour), as well as providing an alert within a day of an interesting outburst. Within 1 kpc ATLAS has a 10σ sensitivity at $M_V = +9$ per visit.

Of course ATLAS will also watch the lesser beasts of the variable zoo in the sky. At 20 kpc ATLAS’s sensitivity at 10σ per day is $M = +3$, so all instability strip stars such as RR Lyrae and Cepheids will have daily observations at high SNR. ATLAS will provide the first opportunity to catalog all the eclipsing and variable binary stars in the sky to $M = +3$ or fainter. ATLAS’s blue filter is deliberately truncated short of $H\alpha$, so ATLAS has special sensitivity to $H\alpha$ flares — variability that is extremely “red” is likely to arise from $H\alpha$.

5.6. Active Galactic Nuclei

Croom et al (2004) analyzed the AGN luminosity function in the SDSS DR5, from which we calculate that there are some half million AGN in the sky brighter than $V = 19.6$. At that level ATLAS can monitor half of them, more than 100,000, at 25σ for a 10 day cadence or 10σ for a daily cadence. AGN have a complex structure function of variability ranging from general flickering of the accretion process to flares from tidal events to the spectacular luminosities of blazars and their instabilities. ATLAS’s sensitivity, solid angle, and cadence has an excellent overlap with the densities of AGN and their various sources of variation. Well sampled light curves with time scales ranging from days to years are key to studying AGN variability.

At $V = 20$ there are 1800 galaxies per square degree, so ATLAS will maintain a daily watch on some 40 million galaxies, sensitive to events whose luminosity is comparable to that of the galaxy on a 1 day timescale or longer. For example, a star is occasionally disrupted by accretion onto a black hole at the center of a galaxy, producing a flare of predictable color and duration. Gezari et al. (2009) predict a volume rate of $2.3 \times 10^{-6} \text{ yr}^{-1} \text{ Mpc}^{-3}$, and calculate that a survey with $g < 19$ would detect events out to 200 Mpc, corresponding to detection rate of 20 events per year by ATLAS.

5.7. Lensing

Even at the north galactic pole there are about 2000 stars per square degree brighter than the 1 day limiting magnitude of $V = 20$. Over the entire 20,000 sq deg being surveyed each night by ATLAS there are about a half billion stars far enough off of the galactic plane that there is manageable confusion in ATLAS’s $4.4''$ pixels.

Han (2008) estimates the rate of near-field microlensing from all sky surveys and finds that at $V = 18$ we can expect to see 23 events per year, where an event is defined as an increase of source flux by more than 0.32 mag. The number scales as $10^{0.4m}$, so at $V = 19$

there should be 58 lensing events over the sky per year. At $V = 18$ the lens-source proper motion can exceed 40 mas yr^{-1} so we could hope to disentangle their light after a few years by imaging from space or ground-based adaptive optics. The event timescales at the fainter limits are about 20 days.

ATLAS will survey half the entire sky at SNR 10 per night at $V = 19.5$, so a $V = 18$ star will be captured with 0.025 mag uncertainty each night and a $V = 19$ star will have 0.06 mag error each night. A 0.3 mag lensing event will therefore be seen at 10σ at $V = 18$ and 5σ at $V = 19$. Over 20 nights, even allowing for weather, ATLAS ought to capture most events to $V < 19$, and the two filters will permit some level of testing of achromaticity. We therefore estimate that ATLAS should see approximately 30 microlensing events in the near-field each year, and 10 should have high signal to noise and time coverage.

There is a suprisingly large cross section for strong gravitational lensing by galaxy centers. We integrated the galaxy velocity dispersion function of Sheth et al. (2003), using both the densities listed for early-type galaxies and late-type galaxy bulges, assuming that each galaxy has an isothermal core capable of lensing. Over the entire sky, the cross section for a lensing magnification of 3 or greater is 0.37 deg^2 for sources at a redshift of $z = 0.5$, 1.75 deg^2 for sources at a redshift of $z = 1.0$, etc, scaling as $(\mu - 1)^{-2}$, where μ is the lensing magnification, and as z^3 in the Euclidean limit. Divided by the $41,250 \text{ deg}^2$ of the sky, this cross section provides a magnification probability.

The number of lensed SNIa that ATLAS will see, even aided by magnification, will barely yield one event per year. Integrating the density of SNIa from Mannucci et al (2007) against the lensing cross section, we expect to see one lensing event per year peaking at a (magnified) magnitude of 20.6. Of course this will be extremely hard to distinguish from the hordes of SNIa close to galaxy centers.

However, the number of magnified AGN that ATLAS will detect is quite large. Integrating the luminosity function of Croom et al. against this cross section gives more than 40 AGN in the sky with a magnification of 3 or larger at a magnitude of 19.6 or brighter (25σ at 10 days, 10σ at 1 day). Among these there are ~ 7 at magnification 10 or greater. The lensing cross section grows rapidly with redshift, of course, so this is an interesting probe of AGN density, AGN variability as a function of redshift, and galaxy core structure as a function of redshift. At high magnifications the microlensing by stars within the lensing galaxy can cause substantial flickering as well.

5.8. The Static Sky

ATLAS has only modest sensitivity on a per-unit telescope basis, and it undersamples a point spread function that will average about $2.5''$ from atmosphere and optics, but the SNR grows as each piece of the sky gets some 350 visits per year (3.1 mag). Figure 5 compares how an 0.01 sq deg piece of sky appears in the digital POSS sky survey, the SDSS sky survey, and ATLAS. ATLAS goes substantially deeper than POSS after a week of observation, even

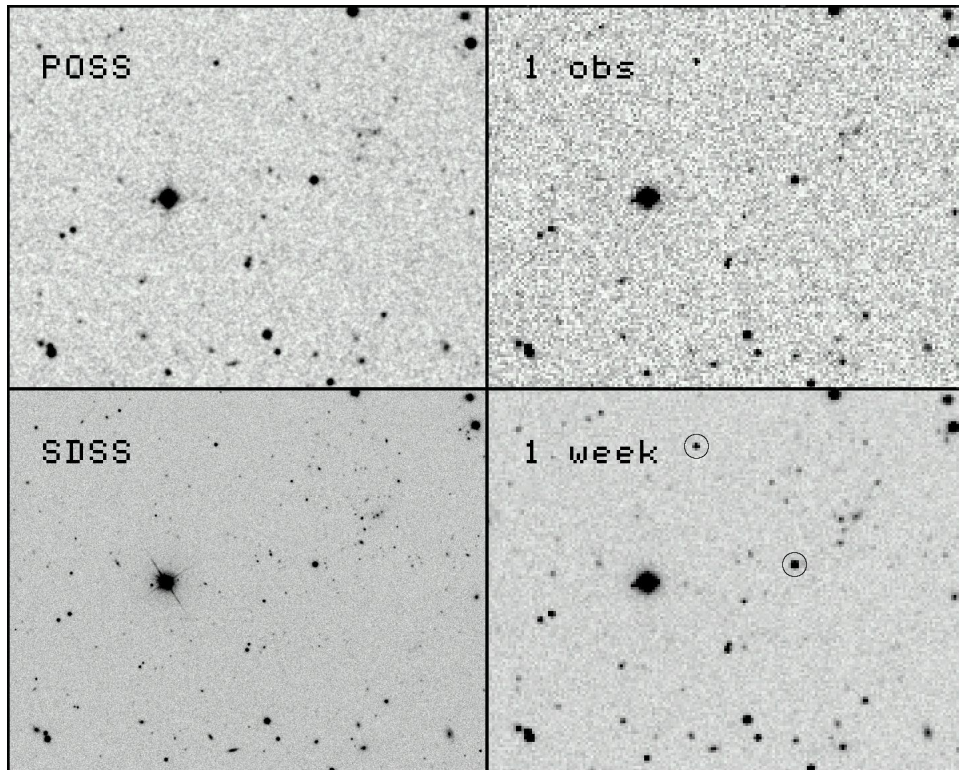


Fig. 5.— The appearance of an 0.1×0.08 deg portion of the sky in POSS R band is shown in the upper left, the view in the SDSS r band in the lower left, how it would appear in a single ATLAS red observation (two 30 sec integrations) in the upper right, and after a week of observation (5 clear nights) in the lower right. The circled stars are $m = 17$, $m = 18.5$, $m = 19.4$ (5σ), and a pair at $m = 18.2$ and 19.2 separated by $4.4''$.

allowing for weather. The SDSS PSF is considerably better than ATLAS can ever achieve, but Figure 6 illustrates how the color co-added sky would look after a year of ATLAS observation (with allowances for weather). After a year’s operation ATLAS is significantly deeper than SDSS (and covers $3/4$ sky), although the coarse sampling eventually runs into

source confusion. However, the density of transient and variable objects is far lower than the density of static objects, so ATLAS should stay above the confusion limit for detection and characterization of the variable parts of their light curves, with sensitivity to timescale τ that goes as $\tau^{1/2}$. For example, ATLAS can achieve $m \sim 23$ sensitivity for slow events such as AGN variability or long-period variable stars.

5.9. Space Junk

There is a growing amount of “space junk” in low Earth orbit (LEO) and geosynchronous Earth orbit (GEO). This is of some concern for satellites and space travel, as evidenced by the recent destruction of an Iridium satellite by collision with a tumbling booster. To sky surveys looking for transients and moving objects, space junk is a significant background signal that masks the solar system objects we are interested in.

A good rule of thumb for the detection of a streak across an image left by a moving object is that when each PSF-sized segment of the streak is 1σ above background it is easily visible to the eye and easily detectable. A magnitude fainter is harder, and two magnitudes

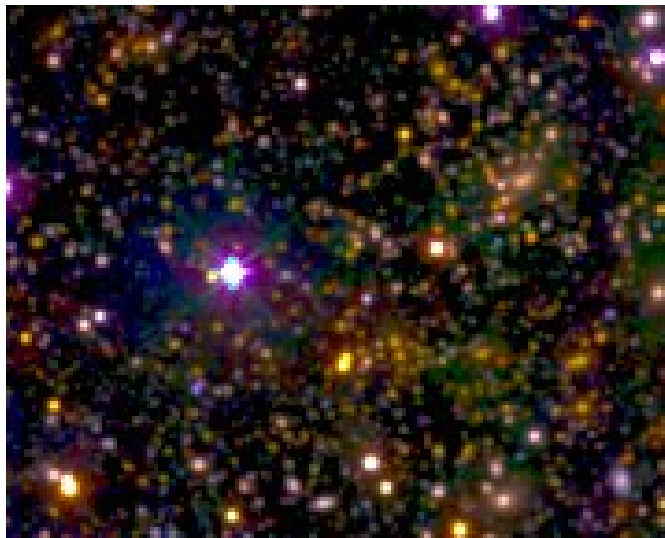


Fig. 6.— A color image of the 0.1×0.08 deg portion of the sky after a year of ATLAS observation illustrates the appearance of SNR 10σ at $V = 22.4$. Although static objects are starting to blend together at this limit, variable objects are rare enough to stand out cleanly once the static sky is subtracted.

fainter is just about the limit of what can be detected.

A LEO object at 1000 km range moves at about 0.4 deg/sec. ATLAS has four views, two staggered by 5 deg at each site and two sites, so many objects will have one or two endpoints caught by the system. A LEO object will spend 3 msec on a pixel, and therefore the 1σ routine detection benchmark is 8.3 mag brighter than the 5σ magnitude limit for a 30 sec exposure, i.e. about $m = 10.8$. At $m = 11.8$ the streak will be visible to the eye and should be possible to detect automatically, particularly given the confirmation from the two sites and the possible collection by the adjacent pointing.

This magnitude corresponds to a white, fully illuminated Lambertian ball of size ~ 4 cm or a piece of space junk of size ~ 15 cm of albedo 0.1 and random illumination. There are estimated to be of order 10,000 objects in LEO of that size or greater.

A GEO object only moves at $15''/\text{sec}$, spending 0.3 sec on a pixel, so the 1-sigma benchmark is 5 mag fainter than LEO, i.e. $m = 15.8$. Automated detection should be possible therefore to $m = 16.8$ (~ 60 cm) without much trouble. At 40,000 km range, the tangential position accuracy should be approximately 100 m, and the range accuracy about 50 km for the single observation. Since ATLAS sweeps the visible sky twice each night, GEO objects will be captured on two occasions, permitting a good estimate of orbit.

6. World-wide Internet Survey Telescope

Apart from its value as a survey for hazardous asteroids, ATLAS also serves to define a unit survey telescope and software that can be replicated many times in order to improve on the networked performance. ATLAS could therefore be a template for a “World-wide Internet Survey Telescope” (WIST) that has as many unit observatories as there are parties who would like to participate, since it is sized to fit within the budget of any college or university.

The ATLAS proposal to NASA is carefully optimized to take advantage of the existing $\sim \$1.3$ M of detectors, tries to avoid as much hardware risk as possible by using commercial components, and plans for software R&D to be the most costly, difficult, and critical aspect of the project. However, given time and resources for hardware R&D, it is possible to develop a successor that would have considerably greater capability per unit cost than the present ATLAS implementation.

For example a remarkable set of designs by M. Akermann, J.T. McGraw, and P.C. Zimmer (private communication) include an 0.5 m aperture Hamilton astrograph with 1 m focal

length and 7 deg FOV that achieves 50% encircled energy at 1.5 μm radius, i.e. half-energy within a diameter of 0.6". The optimal unit camera could have 5–9 μm pixels (0.5–0.2 Gpixel total) for a 1–1.8" sampling over a field of view of ~ 40 sq deg. We note the growing availability of large format detectors, such as the STA-1600 CCD (www.sta-inc.net) that has $10 \times 10\text{k}$ 9 μm pixels and can read out at 1 frame per second, Canon's recent announcement of an APS-H format (29×20 mm), 120 Mpixel CMOS sensor as well as a monolithic 202×205 mm, high-sensitivity sensor, and advances in back-illuminated CMOS detectors by Cypress, Sony, and others. It is not inconceivable that improvements in capability per unit cost of a factor of three or more might emerge.

We have therefore tried to think of ATLAS as the start of a "franchise" that defines what a hardware and software unit should be, basically a high performance telescope and detector system in a robotic observatory, with common reduction and analysis pipeline and common protocols for communications. An essential component is bandwidth management – the ATLAS system has enough local processing to handle the $\sim 100\text{GB}$ per night of raw data, and depends on extra-observatory bandwidth primarily for trading object catalogs that will be orders of magnitude less information.

The Las Cumbres Observatory Global Telescope (Brown et al. 2006) consists of a widely distributed set of many telescopes that are intended for full-time synoptic coverage of interesting events such as planet occultations or microlensing passages. WIST differs by being dedicated to all-sky, nightly survey and discovery. WIST and LCOGT are therefore complementary in their approaches and scientific goals, although both are striving to make the greatest possible use of the silicon revolution and the internet.

Because we want to achieve the highest possible hardware and software performance, and also because we cannot cope with the difficulties inherent in a "National Virtual Observatory" that tries to accept information of varying quality and provenance, the "WIST franchise" would insist on a very high degree of standardization. This does not mean that a college with poor seeing or bright skies cannot participate. WIST is intended to be tolerant of poor seeing, and the standardization allows us to emplace metrics that permit optimal combination of information from all sites.

As the number of observatories grows it would become possible to schedule dynamically according to weather, and to allocate observations by filter or time to different places. Sites with very bright sky backgrounds might be assigned very short exposure times for a more rapid cadence on bright objects, for example. Obviously the search for approaching impactors can be significantly improved by WIST, by virtue of closing the southern blind spot, squeezing down the solar blind spot, immunity to weather, and by deeper imagery.

Since we intend that the cost of WIST be borne by the participants, we expect that all results would be made public immediately. This will encourage participants to define and carry out projects promptly, and we hope will encourage collaborations. The fact that WIST puts the smallest colleges on the same footing with the most prestigious research universities will serve to foster innovation and reduce the dependence of research achievement on availability of resources.

7. Conclusion

In this article we have argued that the congressional mandate to NASA to mitigate the hazard from asteroid impact on Earth can be parsed temporally as well as by impactor size. To some degree the risk can never be reduced to zero because orbits are continually perturbed, but we believe that the most important *time interval* for discovery of small impactors is just before impact, and we have demonstrated that it is relatively easy and cost-effective to patrol that portion of hazard space.

In order to understand the real capability of survey systems we examined the meaning of “etendue” and survey capability, and derived equations that quantify survey capability both in terms of hardware specifications of aperture, solid angle, efficiency, and image quality, but also in terms of actual performance. In support of this we also derived an equation that quantifies the image performance in terms of an “effective noise footprint”, valid even in the regime of pixels that undersample the PSF.

We advanced a description of a new survey instrument, called the “Asteroid Terrestrial-impact Last Alert System”. ATLAS surveys 20,000 sq deg twice per night to magnitude 20, the sensitivity determined by the practical need for three week’s warning of a 100 Mton impact, and the solid angle determined by the practical need for immediate warning of a 1 Mton impact. The components for an ATLAS system are mostly available commercially, the cost is low, and the construction time short.

We compared ATLAS with the other prominent sky-surveys in operation or being planned, and found that ATLAS has interesting complementarities to the other surveys that make it particularly potent for early warning of impacts by hazardous objects: it surveys essentially the entire sky at a rapid cadence so the probability of any object slipping through is reasonably low and its sensitivity is high enough to provide a useful warning. No other survey is as effective for this particular job.

Of course the ATLAS imagery will also open an interesting window on the entire transient universe. Some of the additional science products that ATLAS will produce include:

- hundreds of light curve points for thousands of asteroids that provide estimates of shape and spin,
- detection of all dwarf planets in the solar system,
- twice per night monitoring of ~ 2000 cataclysmic variables,
- detection of ~ 30 near-field microlensing events per year,
- twice per night light curves of most variable stars in the Galaxy,
- novae and luminous blue variable outbursts in most nearby galaxies,
- detailed and prompt information on E&M counterparts to gravity wave events,
- detection of ~ 10 core collapse SN in low metallicity galaxies per year,
- light curves of ~ 4000 SNIa per year with $z < 0.1$, ~ 300 with $V < 17$, and
- variability of $\sim 100,000$ AGN.

We ended with consideration of a future “World-wide Internet Survey Telescope” (WIST), comprised of a confederation of many basic observatory units. The intent is to “franchise” the hardware and software design, but at a cost point that makes an observatory unit affordable by essentially any college or university. This standardization is necessary to allow the full system to be scheduled and for the results of the imagery to be optimally combined, but leads to a system that is virtually unbounded in its ability to explore the time and sensitivity domain of the transient universe.

We acknowledge useful discussions with Christopher Stubbs, Robert Jedicke, Armin Rest, and John Blakeslee. We are grateful for the remarkable design work of Mark Ackermann, John McGraw, and Peter Zimmer. This paper benefited from discussions at the Aspen Center for Physics. Support for this work was provided by National Science Foundation grant AST-1009749.

REFERENCES

- Abadie, J. et al. 2010, *Classical and Quantum Gravity*, 27, 17, 173001
- Asphaug, E. 2009, *Annual Reviews Earth and Planetary Science*, 37, 413
- Bakos, G., et al. 2009, *IAU Symposium*, 253, 354
- Boslough, M.B.E. & Crawford, D.A. 2008, *J. Impact Engineering*, 35, 1441
- Bottke, W. F., Morbidelli, A., Jedicke, R., Petit, J.-M., Levison, H. F., Michel, P., & Metcalfe, T. S. 2002, *Icarus*, 156, 399
- Brown, M. E., Bouchez, A. H., & Griffith, C. A. 2002, *Nature*, 420, 795

- Burgett, W., & Kaiser, N. 2009, Proceedings of the Advanced Maui Optical and Space Surveillance Technologies Conference, held in Wailea, Maui, Hawaii, September 1-4, 2009, Ed.: S. Ryan, The Maui Economic Development Board., p.E39
- Croom, S. M., Smith, R. J., Boyle, B. J., Shanks, T., Miller, L., Outram, P. J., & Loaring, N. S. 2004, MNRAS, 349, 1397
- Gezari, S., et al. 2009, ApJ, 698, 1367
- Han, C. 2008, ApJ, 681, 806
- Ivezic, Z., Tyson, J. A., Allsman, R., Andrew, J., Angel, R., & for the LSST Collaboration 2008, arXiv:0805.2366
- Keller, S. C., et al. 2007, Publications of the Astronomical Society of Australia, 24, 1
- Larson, S., Beshore, E., Hill, R., Christensen, E., McLean, D., Kolar, S., McNaught, R., & Garradd, G. 2003, Bulletin of the American Astronomical Society, 35, 982
- Larsen, J., Roe, E., Albert, E., Descour, A., McMillan, R., Gleason, A., Jedicke, R., Block, M., Bressi, T., Cochran, K., Gehrels, T., Montani, J., Perry, M., Read, M., Scotti, J., and Tubbiolo A. 2007, AJ, 133, 1247
- Law, N. M., et al. 2009, PASP, 121, 1395
- Li, W., Filippenko, A. V., Chornock, R., & Jha, S. 2003, PASP, 115, 844
- McMillan, R. S., and the Spacewatch Team 2006, Proceedings of the International Astronomical Union, Volume 2, Symposium S236, August 2006, “Near Earth Objects, our Celestial Neighbors, Opportunity and Risk”, Published online by Cambridge University Press 03 May 2007. Edited by: Andrea Milani, University degli Studi, Pisa; Giovanni B. Valsecchi, University degli Studi Roma Tre; David Vokrouhlicky, Charles University, Prague, pp 329-340
- Malek, K., et al. 2009, Proceedings of the SPIE, Vol. 7502
- Mannucci, F., Della Valle, M., & Panagia, N. 2007, MNRAS, 377, 1229
- Melosh, H.J. & Collins, G.S. 2005, Nature, 434, 157
- Morbidelli, A. et al. 2002, Icarus, 158, 329
- NASA NEO Report 2007, http://www.nasa.gov/pdf/171331main_NEO_report_march07.pdf

- NRC Report, 2010, “Defending Planet Earth: Near-Earth Object Surveys and Hazard Mitigation Strategies”, National Academies Press, ISBN 0-309-14969
- Ott, C.D. 2009, *Classical and Quantum Gravity*, 26, 6, 063001
- Pollacco, D. L., et al. 2006, *PASP*, 118, 1407
- Sheth, R. K., et al. 2003, *ApJ*, 594, 225
- Schechter, P., Mateo, M., and Saha, A., 1993, *PASP*, 105, 1342
- Stokes, G. H., Evans, J. B., Viggh, H. E. M., Shelly, F. C., & Pearce, E. C. 2000, *Icarus*, 148, 21
- Stubbs, C. W. 2008, *Classical and Quantum Gravity*, 25, 184033
- Trujillo, I., Aguerri, J. A. L., Cepa, J., & Gutiérrez, C. M. 2001, *MNRAS*, 328, 977
- Vereš, P., Jedicke, R., Wainscoat, R., Granvik, M., Chesley, S., Abe, S., Denneau, L., & Grav, T. 2009, *Icarus*, 203, 472
- Vestrand, W. T., Albright, K., Casperson, D., Fenimore, E., Ho, C., Priedhorsky, W., White, R., & Wren, J. 2003, *Gamma-Ray Burst and Afterglow Astronomy 2001: A Workshop Celebrating the First Year of the HETE Mission*, 662, 550
- Young, D. R., Smartt, S. J., Mattila, S., Tanvir, N. R., Bersier, D., Chambers, K. C., Kaiser, N., & Tonry, J. L. 2008, *A&A*, 489, 359